Tokyo Climate Center, Japan Meteorological Agency

TCC News

No. 44 Spring 2016

Contents	Page

El Niño Outlook (May 2016 – November 2016)

It is likely that the current El Niño event will end in spring and La Niña conditions will develop in summer. ***(This article was written based on El Niño outlook issued on 12 May 2016.)***

El Niño/La Niña

In April 2016, the NINO.3 SST was above normal with a deviation of +0.8°C, which was 0.8°C lower than the corresponding figure for March. The five-month running mean of the NINO.3 SST deviation was +0.5°C or above for 21 consecutive months up to February. SSTs (Figures 1 and 3 (a)) were remarkably above normal in the central equatorial Pacific in April, and close to normal in the eastern part, where below normal values were also observed in some areas. Subsurface temperatures were below normal in almost whole regions from the western to the eastern part of the equatorial Pacific (Figures 2 and 3 (b)). Atmospheric convective activity was above normal near the date line in the equatorial Pacific, and easterly winds in the lower troposphere (known as trade winds) were weaker than normal. These atmospheric conditions were consistent with common patterns observed in past El Niño events, while the oceanic conditions indicate a decay of the current El Niño conditions.

The subsurface cold waters observed in April from the western to the eastern equatorial Pacific are expected to migrate eastward in the months ahead, and a tendency toward even cooler-than-normal sea surface conditions will be seen in the eastern equatorial Pacific. Outputs from JMA's El Niño prediction model suggests that the NINO.3 SST will be below normal in boreal summer and autumn (Figure 4). In conclusion, it is likely that the current El Niño event will end in spring, and La Niña conditions will develop in summer.

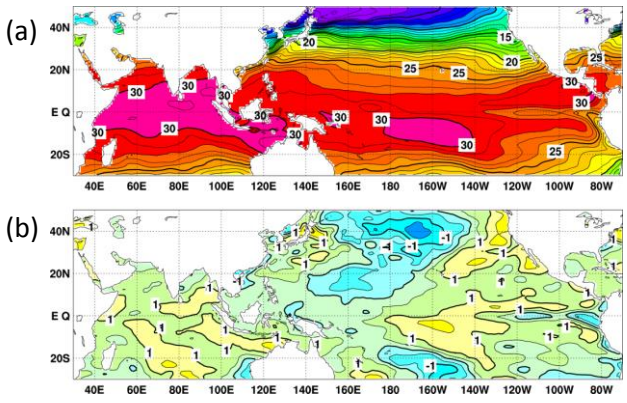

Figure 1 Monthly mean (a) sea surface temperatures (SSTs) and (b) SST anomalies in the Indian and Pacific Ocean areas for April 2016

The contour intervals are 1˚C in (a) and 0.5˚C in (b). The base period for the normal is 1981 – 2010.

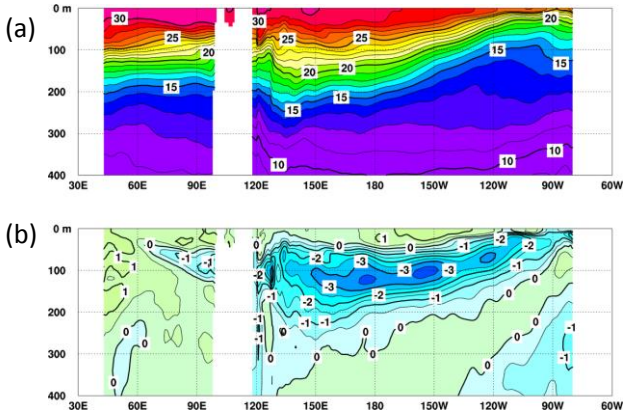

Figure 2 Monthly mean depth-longitude cross sections of (a) temperatures and (b) temperature anomalies in the equatorial Indian and Pacific Ocean areas for April 2016

The contour intervals are 1˚C in (a) and 0.5˚C in (b). The base period for the normal is 1981 – 2010.

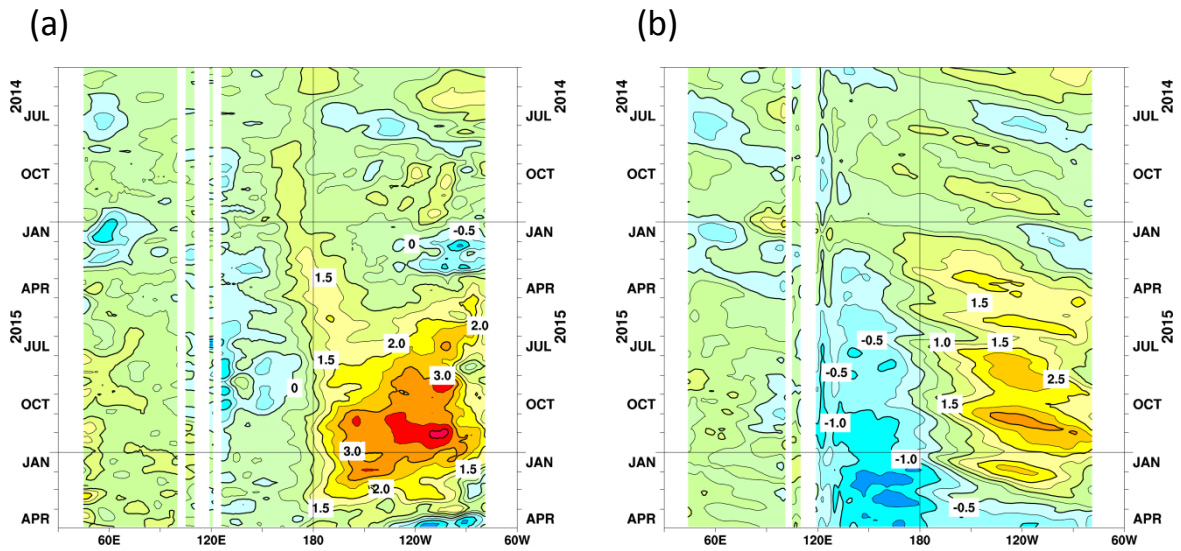

Figure 3 Time-longitude cross sections of (a) SST and (b) ocean heat content (OHC) anomalies along the equator in the Indian and Pacific Ocean areas

OHCs are defined here as vertical averaged temperatures in the top 300 m. The base period for the normal is 1981 – 2010.

Western Pacific and Indian Ocean

The area-averaged SST in the tropical western Pacific (NINO.WEST) region was below normal in April, and is likely to be above normal in boreal summer and autumn.

The area-averaged SST in the tropical Indian Ocean (IOBW) region was above normal in April. The value is likely to remain above normal until boreal summer to move gradually closer to normal in autumn.

Impacts

The ongoing El Niño conditions are considered to have caused the warmer-than-normal conditions observed from Eastern Japan to Okinawa-Amami and as well as the wetter-than-normal conditions and the shorter-than-normal sunshine durations observed in Western Japan in April 2016.

In the same month, warmer-than-normal conditions in West Africa, regions near Madagascar, the southern part of India, Southeast Asia, and the eastern part of Australia were consistent with common patterns observed in past El Niño events.

(Ichiro Ishikawa, Climate Prediction Division)

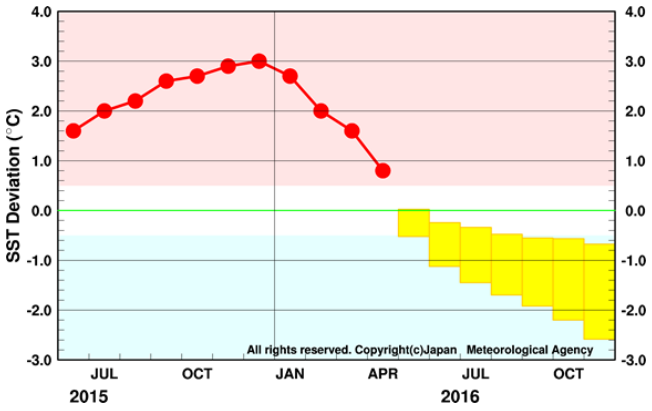

Figure 4 Outlook of NINO.3 SST deviation produced by the El Niño prediction model

This figure shows a time series of monthly NINO.3 SST deviations. The thick line with closed circles shows observed SST deviations, and the boxes show the values produced for up to six months ahead by the El Niño prediction model. Each box denotes the range into which the SST deviation is expected to fall with a probability of 70%.

* The SST normal for the NINO.3 region (5°S - 5°N, 150°W - 90°W) is defined as an monthly average over a sliding 30-year period (1985-2014 for this year).

* The SST normals for the NINO.WEST region (Eq. - 15°N, 130°E - 150°E) and the IOBW region (20°S - 20°N, 40°E - 100°E) are defined as linear extrapolations with respect to a sliding 30-year period, in order to remove the effects of significant long-term warming trends observed in these regions.

JMA's Seasonal Numerical Ensemble Prediction for Boreal Summer 2016

Based on JMA's seasonal ensemble prediction system, sea surface temperature (SST) anomalies are predicted to be below normal in the equatorial eastern Pacific Ocean during this boreal summer, suggesting a likely transition to La Niña conditions. Conversely, SST anomalies are predicted to be above normal in the Indian Ocean. In association with warm SST conditions, active convection is predicted over the Indian Ocean. Conversely, inactive convection is predicted over the western Pacific Ocean.

1. Introduction

This article outlines JMA's dynamical seasonal ensemble prediction for boreal summer 2016 (June – August, referred to as JJA), which was used as a basis for JMA's operational warm-season outlook issued on 25 May 2016. The outlook is based on the seasonal ensemble prediction system of the Coupled Atmosphere-ocean General Circulation Model (CGCM). See the column below for system details.

Section 2 outlines global SST anomaly predictions, and Section 3 describes the associated circulation field predictions for the tropics and sub-tropics. Finally, the circulation fields predicted for the mid- and high latitudes of the Northern Hemisphere are discussed in Section 4.

2. SST anomalies (Figure 5)

Figure 5 shows predicted SSTs (contours) and related anomalies (shading) for JJA. Below normal anomalies are predicted in the equatorial eastern Pacific Ocean throughout the period, suggesting a likely transition to La Niña conditions. Conversely, above normal anomalies are predicted in the Indian Ocean, reflecting the Indian Ocean Capacitor Effect which is well observed in post El Niño years.

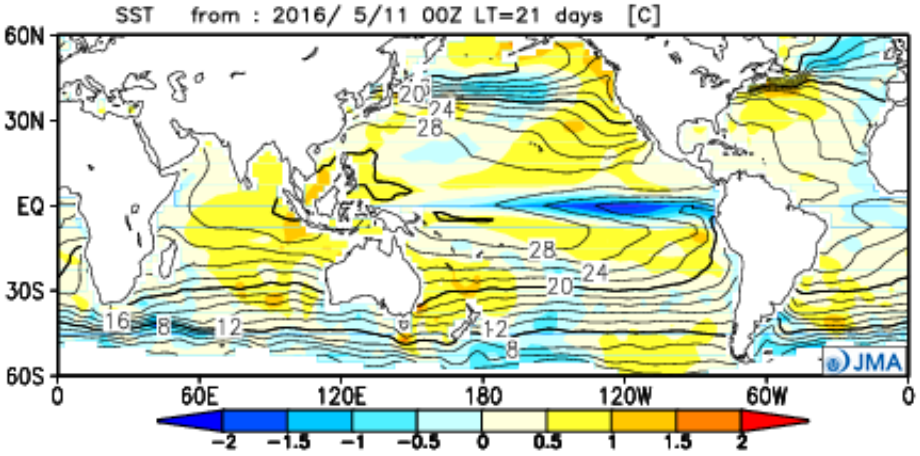

Figure 5
Predicted SSTs (contours) and SST anomalies (shading) for June–August 2016 (ensemble mean of 51 members)

3. Prediction for the tropics and sub-tropics (Figure 6)

Figure 6 (a) shows predicted precipitation (contours) and related anomalies (shading) for JJA. In association with warm SST conditions, above normal anomalies are predicted over the Indian Ocean. At the same time, it is likely that the summer monsoon will be more active than normal years in South Asia. Conversely, below normal anomalies are predicted over the western Pacific Ocean and the Indochina Peninsula. Accordingly, it is likely that the summer monsoons will be more inactive than normal years in those regions.

Figure 6 (b) shows predicted velocity potential (contours) and related anomalies (shading) at the upper troposphere (200hPa) for JJA. Negative (i.e., divergent) anomalies are predicted over the Indian Ocean in association with active convection. Conversely, positive (i.e., convergent) anomalies are predicted over the western Pacific Ocean in association with inactive convection. These are consistent with the typical atmospheric circulation pattern well observed in association with the Indian Ocean Capacitor Effect.

Figure 6 (c) shows predicted stream functions (contours) and related anomalies (shading) at the upper troposphere (200hPa) for JJA. Negative anomalies (i.e., cyclonic) are predicted in Southeast Asia in association with inactive convection over the western Pacific Ocean, suggesting a weak Tibetan High over those regions. Conversely, positive anomalies (i.e., anticyclonic) are predicted over West Asia in association with active convection over the Indian Ocean.

Figure 6 (d) shows predicted stream functions (contours) and related anomalies (shading) at the lower troposphere (850hPa) for JJA. Equatorial symmetric anticyclonic anomalies are predicted over the Maritime Continent in association with inactive convection over the western Pacific Ocean. Conversely, equatorial symmetric cyclonic anomalies are predicted over the western Indian Ocean in association with active convection over the Indian Ocean.

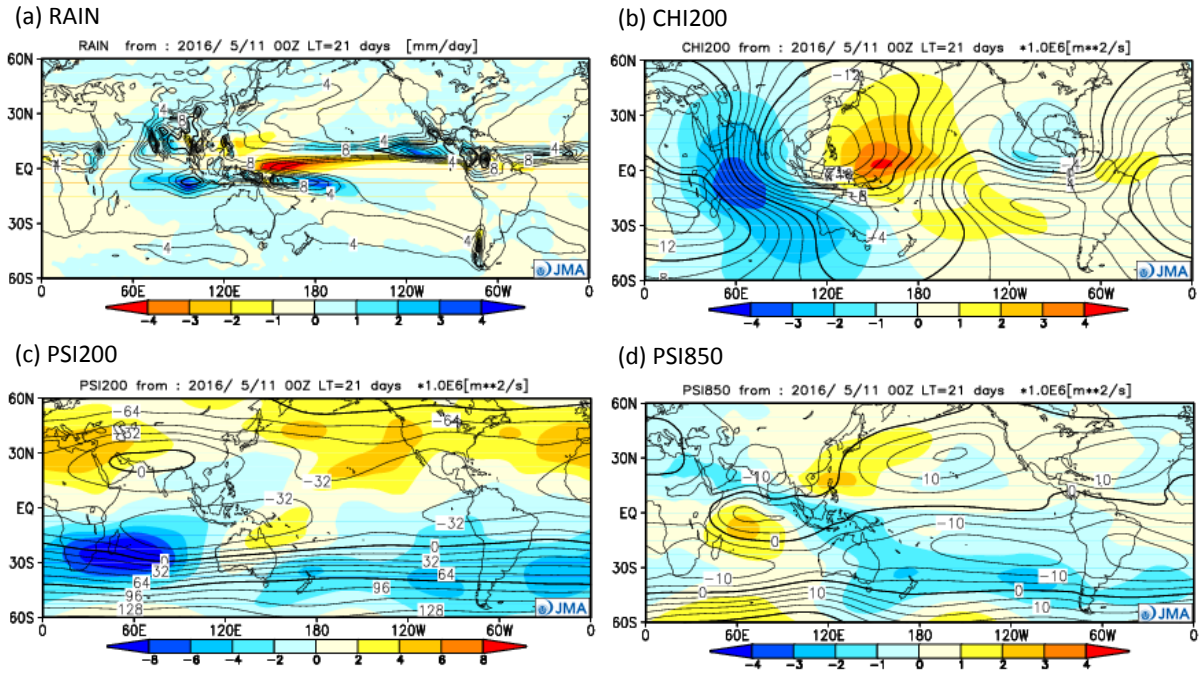

Figure 6 Predicted atmospheric fields from 60°N – 60°S for June–August 2016 (ensemble mean of 51 members)

(a) Precipitation (contours) and anomaly (shading). The contour interval is 2 mm/day.
(b) Velocity potential at 200 hPa (contours) and anomaly (shading). The contour interval is 2×10^6 m^2/s.
(c) Stream function at 200 hPa (contours) and anomaly (shading). The contour interval is 16×10^6 m^2/s.
(d) Stream function at 850 hPa (contours) and anomaly (shading). The contour interval is 5×10^6 m^2/s.

4. Prediction for the mid- and high- latitudes of the Northern Hemisphere (Figure 7)

Figure 7 (a) shows predicted geopotential heights (contours) and related anomalies (shading) at 500hPa for JJA. Positive anomalies are predicted over most of the Northern Hemisphere, suggesting a high thickness in association with post El Niño conditions and a global warming trend.

Figure 7 (b) shows predicted sea level pressure (contours) and related anomalies (shading) for JJA. Positive anomalies are predicted over the northwestern Pacific Ocean, suggesting a stronger North Pacific High than normal.

(Takashi Yamada, Climate Prediction Division)

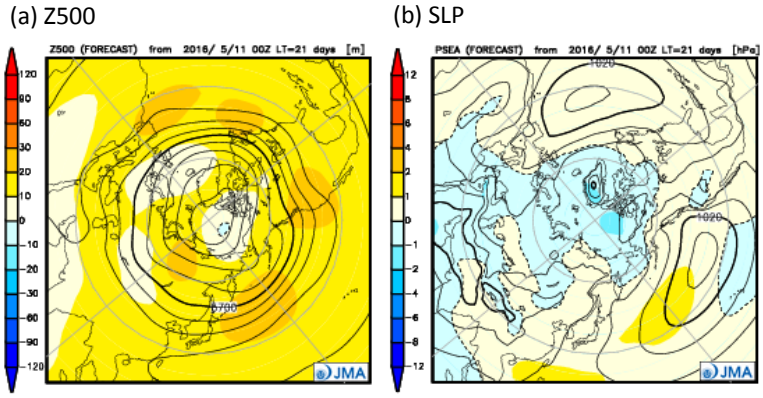

Figure 7 Predicted atmospheric fields from 60°N - 60°S for June–August 2015 (ensemble mean of 51 members)

(a) Geopotential height at 500hPa (contours) and anomaly (shading). The contour interval is 60 m.
(b) Sea level pressure (contours) and anomaly (shading). The contour interval is 4hPa.

JMA's Seasonal Ensemble Prediction System

JMA operates a seasonal Ensemble Prediction System (EPS) using the Coupled atmosphere-ocean General Circulation Model (CGCM) to make seasonal predictions beyond a one-month time range. The EPS produces perturbed initial conditions by means of a combination of the initial perturbation method and the lagged average forecasting (LAF) method. The prediction is made using 51 members from the latest four initial dates (thirteen members are run every five days). Details of the prediction system and verification maps based on 30-year hindcast experiments (1981–2010) are available at http://ds.data.jma.go.jp/tcc/tcc/products/model/.

Warm Season Outlook for Summer 2016 in Japan

In February 2016, JMA issued its outlook for the coming summer (June – August) for Japan and updated it in March and April based on output from its seasonal Ensemble Prediction System (EPS). This article outlines the update of 25 April.

1. Outlook summary (Figure 8)

- In northern, eastern and western Japan, warm-season precipitation amounts are expected to be above normal due to significant influence from active fronts and southerly wet flows.
- In western Japan and Okinawa/Amami, seasonal mean temperatures are expected to be above normal.
- In midsummer after the rainy season (Baiu), below-normal numbers of sunny days are expected in northern and eastern Japan, while above-normal numbers are expected in Okinawa/Amami.

2. Outlook background

Figure 9 shows a conceptual diagram highlighting expected large-scale ocean/atmosphere characteristics for summer. An outline of the background to the outlook is given below.

- Sea surface temperatures (SSTs) in the eastern tropical Pacific are expected to be near or below normal in the Northern Hemisphere in summer. Accordingly, the development of La Niña conditions during summer in the Northern Hemisphere is more likely than a continuation of ENSO-neutral conditions. Meanwhile, SSTs over the tropical Indian Ocean (IO) are expected to be above normal.
- In association with expected SST anomalies in the tropics, convection in the tropics is expected to be more active than normal over the Indian Ocean and less active than normal over the Southeast Asian monsoon region.
- The Tibetan High is expected to be weaker than normal in association with inactive convection over the Southeast Asian monsoon region. Accordingly, the subtropical jet stream, which flows along the northern edge of the Tibetan High, is expected to shift southward of its normal position from the Eurasian continent to the area east of Japan.
- Expansion of the North Pacific High is expected to be stronger than normal to its western part (i.e., from the southern part of Japan to Okinawa/Amami) and weaker than normal to its northern part (i.e., around northern Japan). As the North Pacific High is likely to be stronger than normal in the south of Japan, wet southerly flows into the front line along its northern edge are expected. This pattern (i.e., the combination of a stronger-than-normal North Pacific High and more frontal activity over the main island of Japan) is similar to the negative phase of the Pacific-Japan teleconnection pattern.

(continued overleaf)

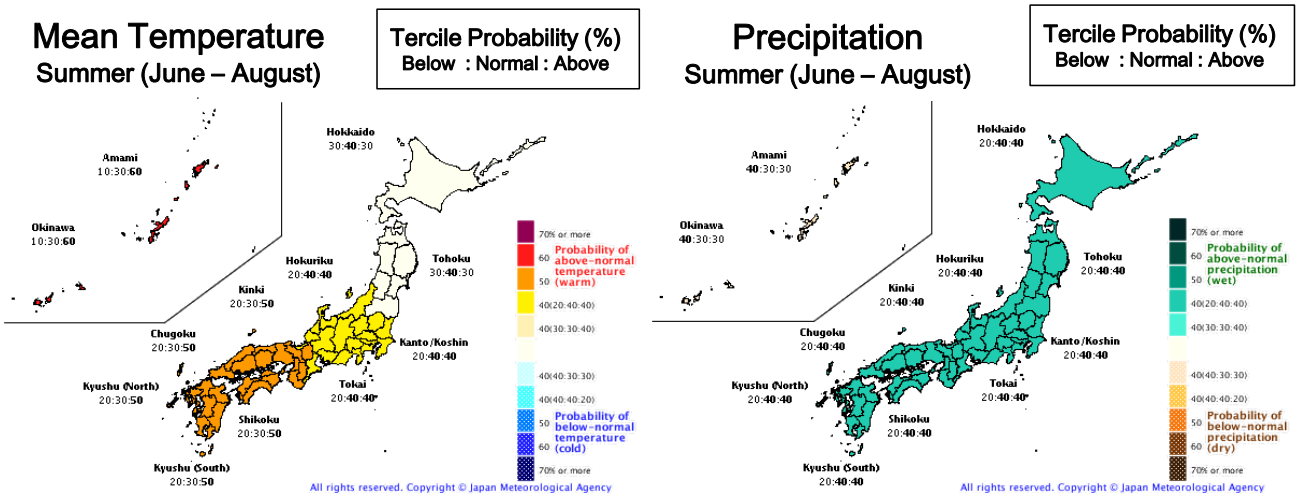

Figure 8 Outlook for summer 2016 temperature (left) and precipitation (right) probability in Japan.

- Overall temperatures in the troposphere are expected to be higher than normal in association with the El Niño event and the prevailing long-term trend. This may increase the likelihood of above-normal temperatures, especially at lower latitudes. Meanwhile, climatological statistics suggest the possible prevalence of the Okhotsk High (which causes cool conditions in northern and eastern Japan) in association with Indian Ocean warming in the post-El Niño stage. Accordingly, forecasters should take account of the significant uncertainty associated with warming-tendency predictions associated with the appearance of the Okhotsk High, especially for northern Japan.
- In consideration of the above, seasonal precipitation is expected to be above normal in northern, eastern and western Japan with 40% probability and near normal in Okinawa/Amami.
- Seasonal mean temperatures are expected to be above normal with 60% probability in Okinawa/Amami, with 50% probability in western Japan and with 40% probability in eastern Japan, and near normal in northern Japan.

(Masayuki Hirai, Climate Prediction Division)

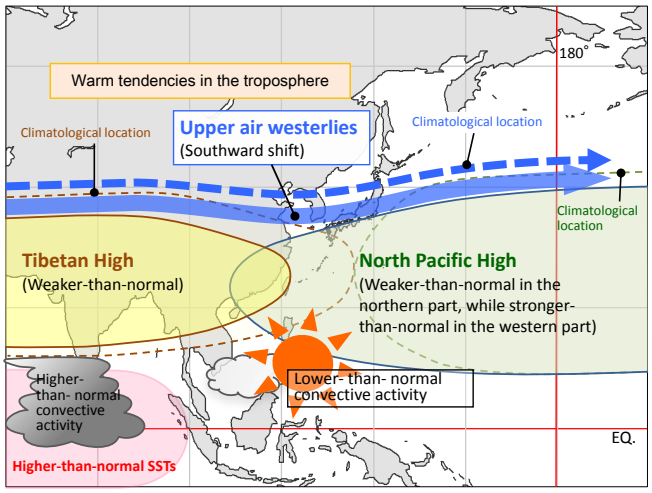

Figure 9 Conceptual diagram showing expected large-scale ocean/atmosphere characteristics for summer 2016

Summary of the 2015/2016 Asian Winter Monsoon

This report summarizes the characteristics of the surface climate and atmospheric/oceanographic considerations related to the Asian winter monsoon for 2015/2016.

Note: The Japanese 55-year Reanalysis (JRA-55; Kobayashi et al. 2015) atmospheric circulation data and COBE-SST (JMA 2006) sea surface temperature (SST) data were used for this investigation. The outgoing longwave radiation (OLR) data referenced to infer tropical convective activity were originally provided by NOAA. The base period for the normal is 1981 – 2010. The term "anomaly" as used in this report refers to deviation from the normal.

1. Surface climate conditions

1.1 Overview of Asia

In boreal winter 2015/2016, general Asian climate characteristics included higher-than-normal temperatures in most lower latitudes as well as above- and below-normal precipitation over southeastern China to Japan and parts of the Maritime Continent, respectively. These conditions were largely consistent with expected El Niño winter patterns. Despite the prominent influence of the El Niño event, a severe cold wave associated with intra-seasonal variability struck East Asia in January.

Temperatures from December 2015 to February 2016 (DJF) were above normal in most parts of Asia and Siberia except for Mongolia and China (Figure 10). This tendency was especially apparent in low-latitude regions, and was consistent with typical anomaly patterns for past El Niño events (Figure 13). Meanwhile, extremely low temperatures were observed in Mongolia and China in January. A strong cold wave in late January was a notable weather characteristic of this boreal winter, which brought record-low temperatures and snowfall. In many regions, daily mean temperatures on January 24 were more than 6 degrees Celsius below normal (Figure 11).

Precipitation amounts averaged over DJF were below normal over the Maritime Continent and India (Figure 12). The dry conditions observed over the Maritime Continent were also consistent with typical anomaly patterns observed in past El Niño events (Figure 13). In most other regions, precipitation amounts were above normal in DJF. However, below-normal monthly precipitation amounts were observed in eastern Siberia in December, western to central Siberia and central to northeastern China in January, and from eastern parts of Central Asia to western China, southeastern China and the Indochina Peninsula in February.

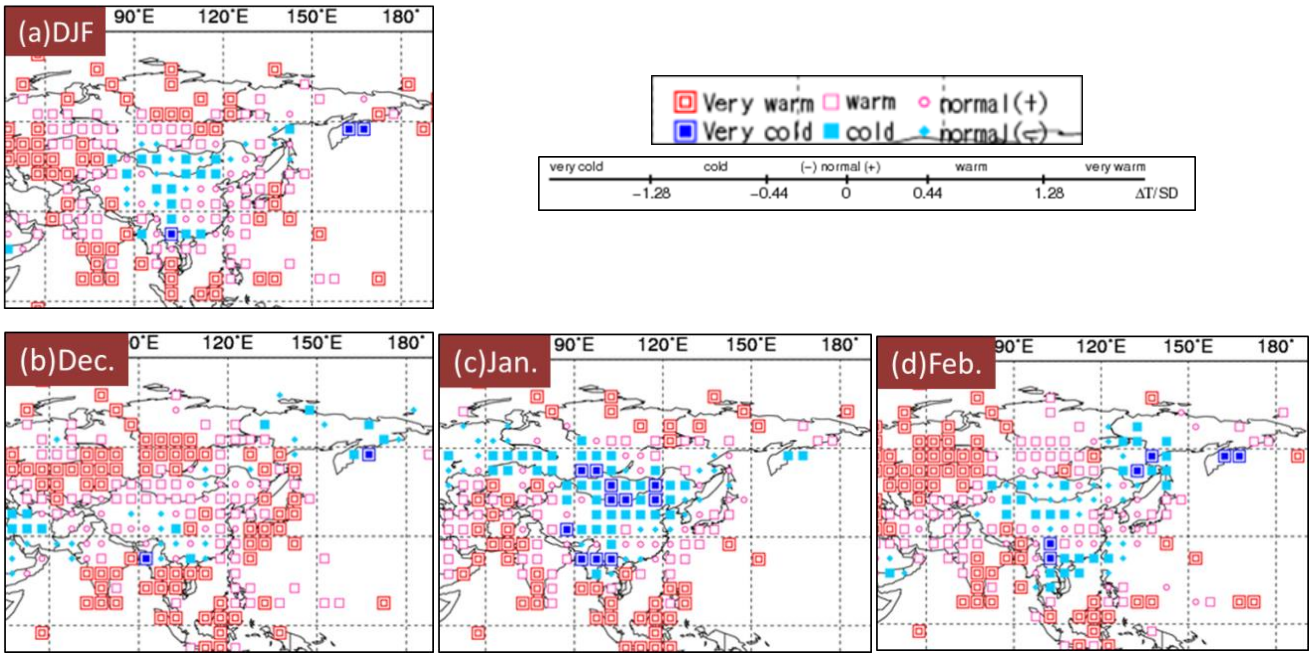

Figure 10 (a) Three-month mean temperature anomalies for December 2015 – February 2016, and monthly mean temperature anomalies for (b) December 2015, (c) January 2016 and (d) February 2016

Categories are defined by the three-month/monthly mean temperature anomaly against the normal divided by its standard deviation and averaged in 5° × 5° grid boxes. The thresholds of each category are -1.28, -0.44, 0, +0.44 and +1.28. Standard deviations were calculated from 1981 - 2010 statistics. Areas over land without graphical marks are those where observation data are insufficient or where normal data are unavailable.

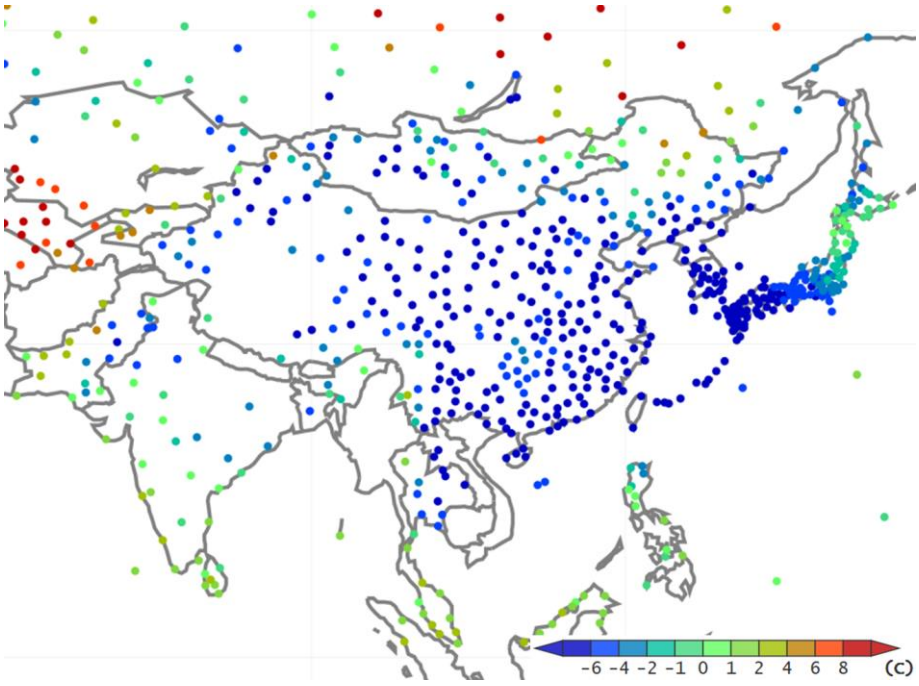

Figure 11 Daily mean temperature anomalies on 24 January 2016 based on SYNOP observation.

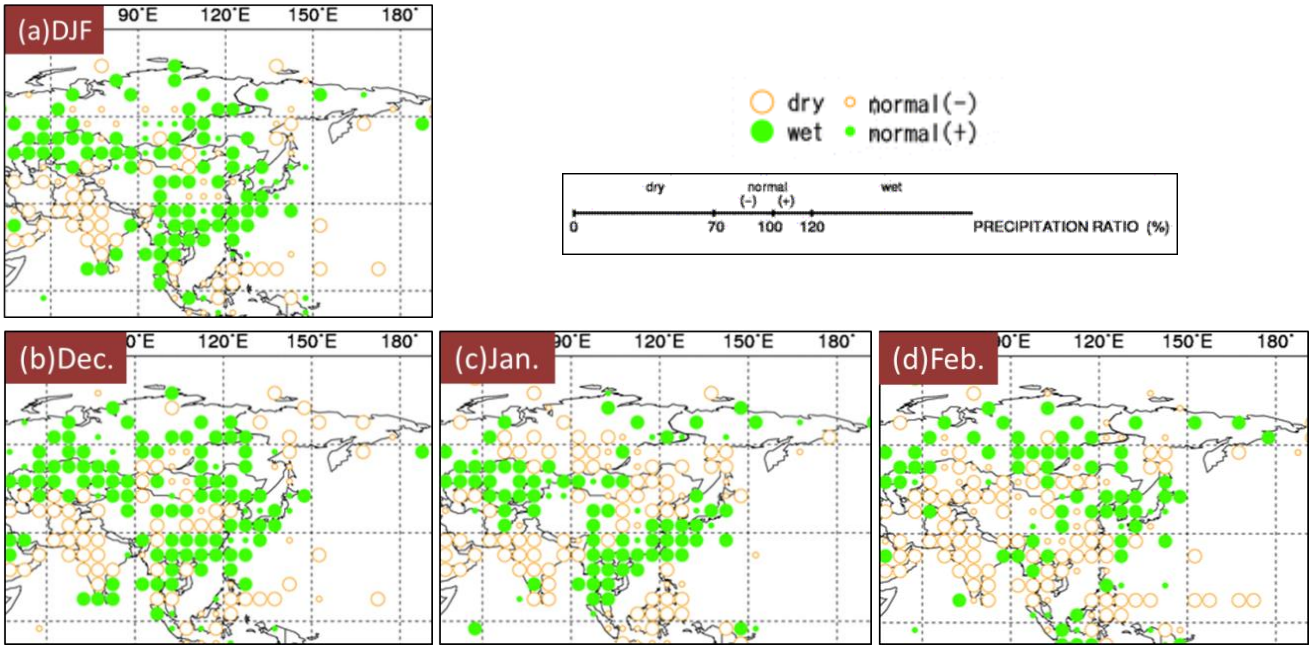

Figure 12 (a) Three-month total precipitation ratio for December 2015 – February 2016, and monthly precipitation ratio for (b) December 2015, (c) January 2016 and (d) February 2016

Categories are defined by the three-month/monthly mean temperature anomaly against the normal divided by its standard deviation and averaged in 5° × 5° grid boxes. The thresholds of each category are 70, 100 and 120%. Areas over land without graphical marks are those where observation data are insufficient or where normal data are unavailable.

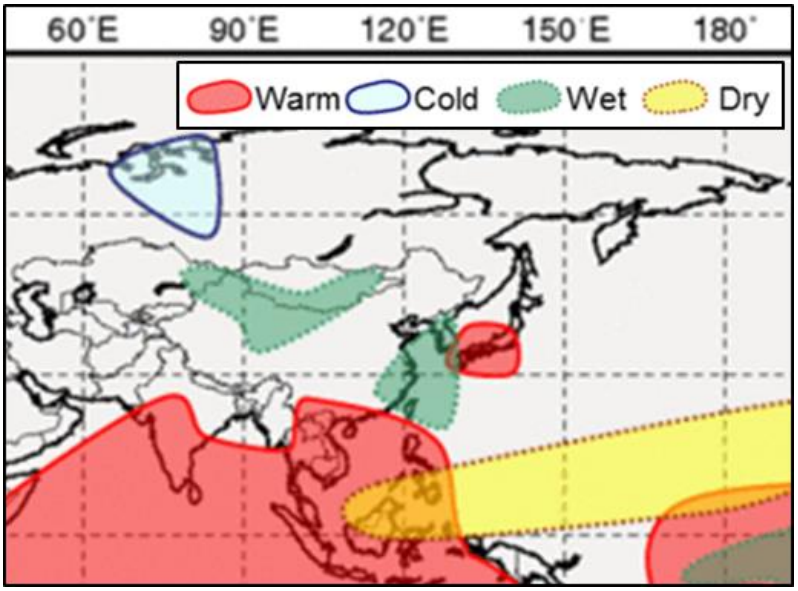

Figure 13 The schematic charts for typical anomaly patterns of surface temperature and precipitation in boreal winter in past El Niño events.

2. Characteristic atmospheric circulation and oceanographic conditions

2.1 Conditions in the tropics and Asian Winter Monsoon

In winter 2015/2016, the El Niño conditions that emerged in summer 2014 peaked. Sea surface temperatures (SSTs) were markedly above normal in the central-to-eastern equatorial Pacific and slightly below normal in tropical latitudes north of the equator in the western Pacific. In the Indian Ocean, SSTs were above normal basin-wide (Figure 14), as usually observed during or immediately after El Niño events. Although an active convection phase of the Madden-Julian Oscillation (MJO) propagated eastward from the eastern Indian Ocean via the Pacific and back to the Indian Ocean from early December to mid-January, eastward propagation of convection anomalies related to the MJO was limited (Figure 15) in association with the significant El Niño episode. Convective activity averaged over the three months from December to February, as well as for individual months, was enhanced over the central-to-eastern equatorial Pacific and suppressed over Southeast Asia (Figure 16).

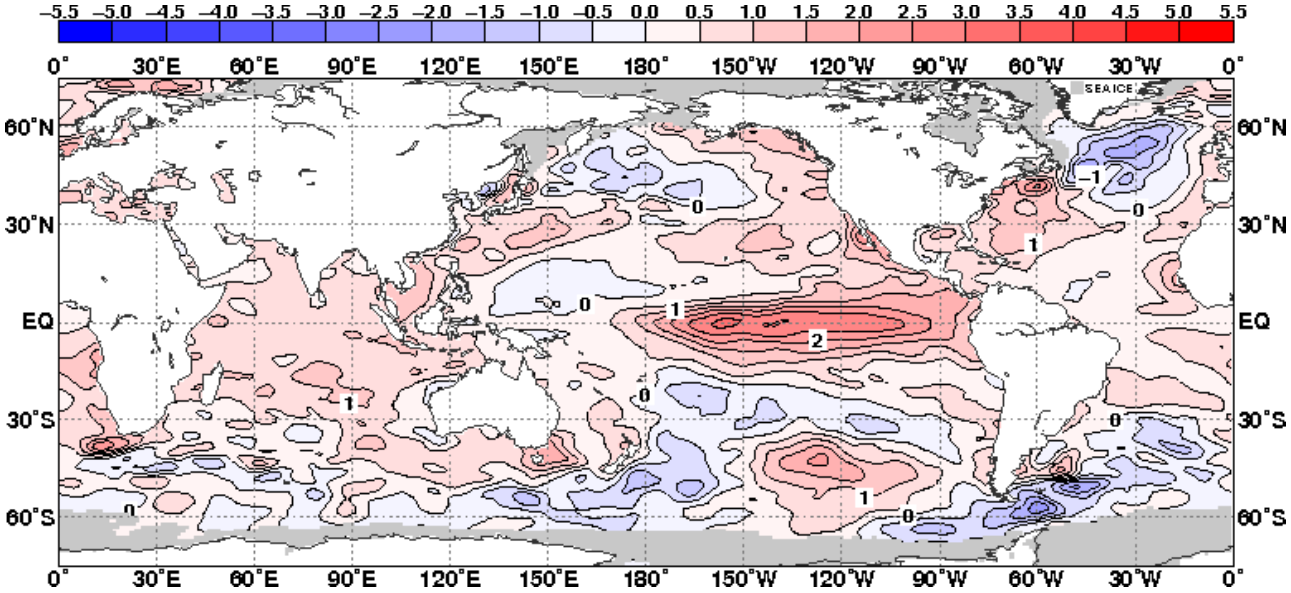

Figure 14 Three-month mean sea surface temperature (SST) anomalies for December 2015 to February 2016
The contour interval is 0.5˚C.

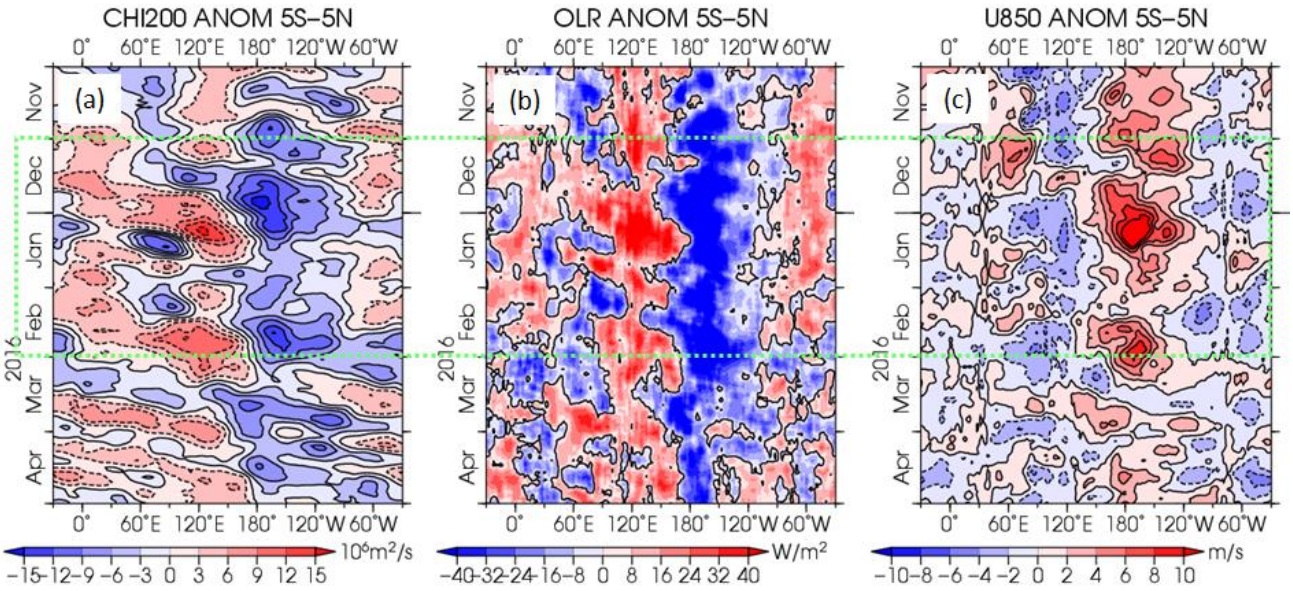

Figure 15 Time-longitude cross section of seven-day running mean (a) 200-hPa velocity potential anomalies, (b) outgoing longwave radiation (OLR) anomalies, and (c) 850-hPa zonal wind anomalies around the equator (5°S – 5°N) for November 2015 to April 2016
(a) The blue and red shading indicate areas of divergence and convergence anomalies, respectively. (b) The blue and red shading indicate areas of enhanced and suppressed convective activity, respectively. (c) The blue and red shading show easterly and westerly wind anomalies, respectively.

2.2 Conditions in atmospheric circulation

In the 200-hPa stream function field (Figure 17 (a)), pronounced cyclonic circulation anomalies were centered over southern China in response to suppressed convective activity over Southeast Asia. Originating from this cyclonic circulation, a wave train pattern was noticeable with anticyclonic anomalies to the east of Japan. In the 850-hPa stream function field (Figure 18 (a)), anticyclonic circulation anomalies were centered over the Philippines and to the east of Japan. In relation, temperatures in the lower troposphere were above normal over and around Japan (Figure 20 (a)). Meanwhile, the Aleutian Low was stronger than normal southeastward of its climatological extension (Figure 21 (a)). Overall, the circulation anomaly pattern detailed above affords close parallels to those observed in past El Niño winters.

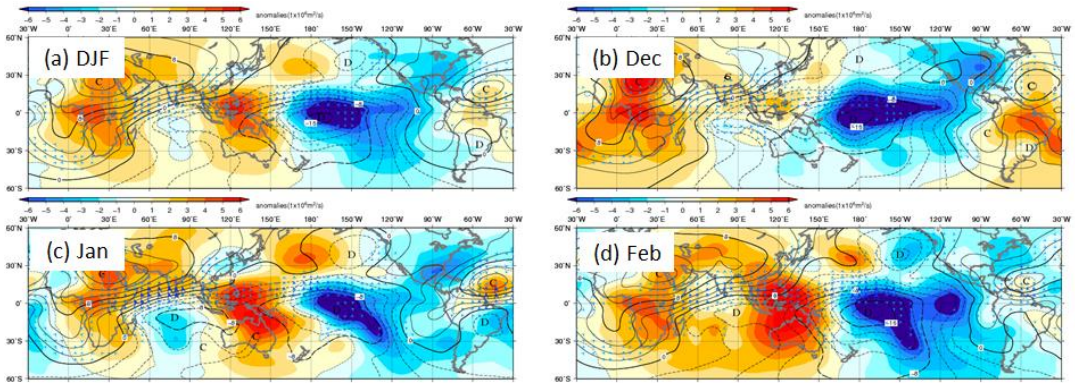

Figure 16 200-hPa velocity potential (a) averaged over the three months from December 2015 to February 2016, for (b) December 2015, (c) January 2016 and (d) February 2016

The contours indicate velocity potential at intervals of 2×10^6 m^2/s, and the shading shows velocity potential anomalies. D and C indicates the bottom and peak of velocity potential, corresponding to the centers of large-scale divergence and convergence, respectively.

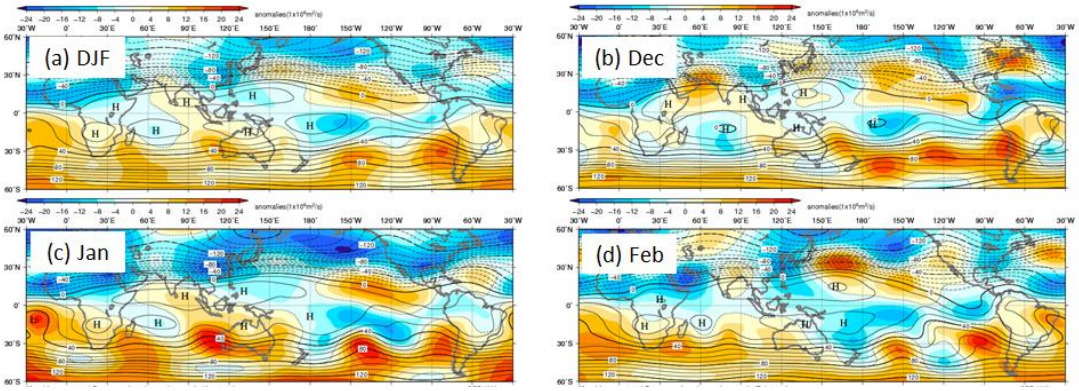

Figure 17 200-hPa stream function (a) averaged over the three months from December 2015 to February 2016, for (b) December 2015, (c) January 2016, and (d) February 2016

The contours indicate stream function at intervals of 10×10^6 m^2/s and the shadings indicate anomalies. H and L denote the centers of anticyclonic and cyclonic circulation anomalies, respectively.

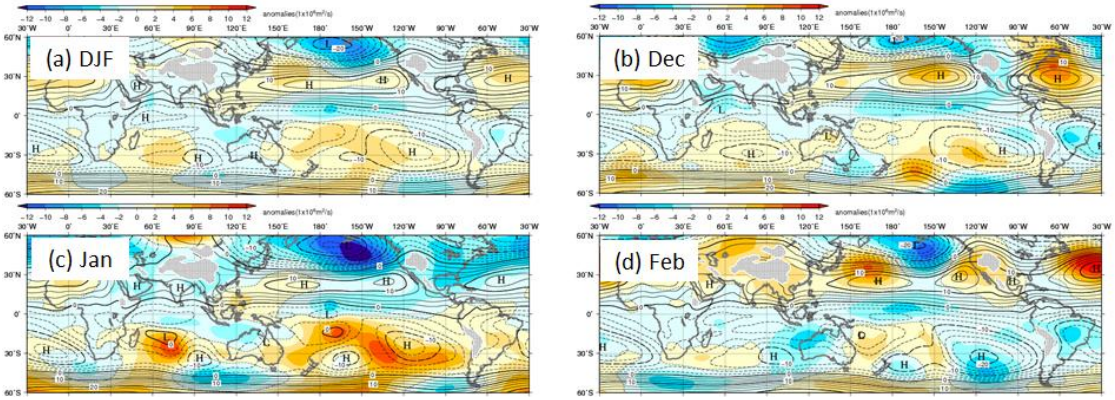

Figure 18 850-hPa stream function (a) averaged over the three months from December 2015 to February 2016, for (b) December 2015, (c) January 2016, and (d) February 2016

The contours indicate stream function at intervals of 2.5×10^6 m^2/s and the shadings indicate anomalies. H and L denote the centers of anticyclonic and cyclonic circulation anomalies, respectively.

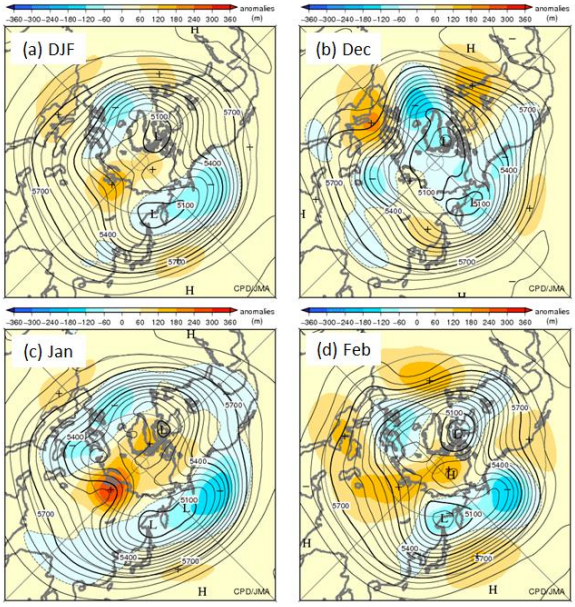

Figure 19 500-hPa height (a) averaged over the three months from December 2015 to February 2016, for (b) December 2015, (c) January 2016, and (d) February 2016

The contours indicate 500-hPa height at intervals of 60 m, and the shading denotes anomalies. H and L indicate the peak and bottom of 500-hPa height, respectively, and + (plus) and – (minus) show the peak and bottom of anomalies, respectively.

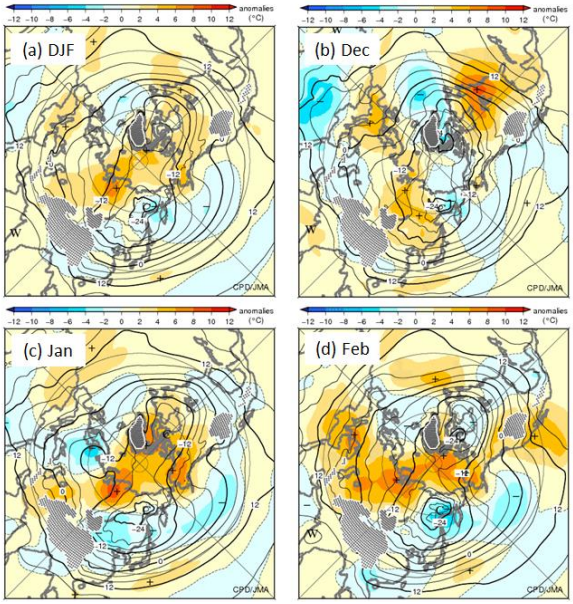

Figure 20 850-hPa temperature (a) averaged over the three months from December 2015 to February 2016, for (b) December 2015, (c) January 2016, and (d) February 2016

The contours indicate 850-hPa temperature at intervals of 4°C, and the shading denotes anomalies. W and C indicate the centers of warm and cold air, respectively, and + (plus) and – (minus) show the peak and bottom of 850hPa temperature anomalies, respectively.

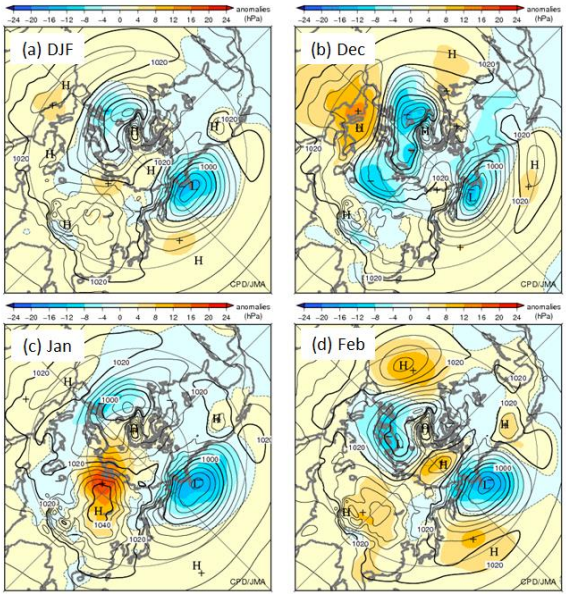

Figure 21 Sea level pressure (a) averaged over the three months from December 2015 to February 2016, for (b) December 2015, (c) January 2016 and (d) February 2016

The contours indicate sea level pressure at intervals of 4 hPa, and the shading shows related anomalies. H and L indicate the centers of high and low pressure systems, respectively, and + (plus) and – (minus) show the peak and bottom of sea level pressure anomalies, respectively.

2.3 Notable events

In December 2015, the 500-hPa height field exhibited positive anomalies over Europe and East Asia and negative anomalies over the North Atlantic and Western Siberia (Figure 19 (b)). This pattern was reminiscent of circulation anomalies representing a negative phase of the Eurasian (EU) teleconnection pattern (Figure 22 (a)). This negative phase is generally linked to a weaker-than-normal Siberian High and higher-than-normal temperatures over East Asia, as observed in December 2015 (Figure 20 (b) and Figure 21 (b)).

The phase of the EU teleconnection sharply reversed in early January and remained positive throughout the month (Figure 22 (b)) with a pronounced ridge centered over the longitude of 90°E and negative height anomalies over Eastern Europe and East Asia (Figure 19 (c)). This was in stark contrast to the circulation pattern dominant in the previous month. In close association with this change, the Siberian High turned stronger than normal (Figure 21 (c)), and temperatures were below normal over large parts of East Asia (Figure 20 (c)).

In late January, positive 500-hPa height anomalies over Western Siberia significantly amplified, and a deep trough concurrently developed over East Asia (Figure 23 (a)). In the lower troposphere between these positive and negative anomalies, the intensity and extension of the Siberian High increased (Figure 23 (b)) to a degree at which its center exhibited a rare sea level pressure exceeding 1,070 hPa. This created a situation in which a large part of East Asia was struck by an exceptional cold wave and experienced extremely low temperatures around January 23 - 24 (Figure 23 (c)).

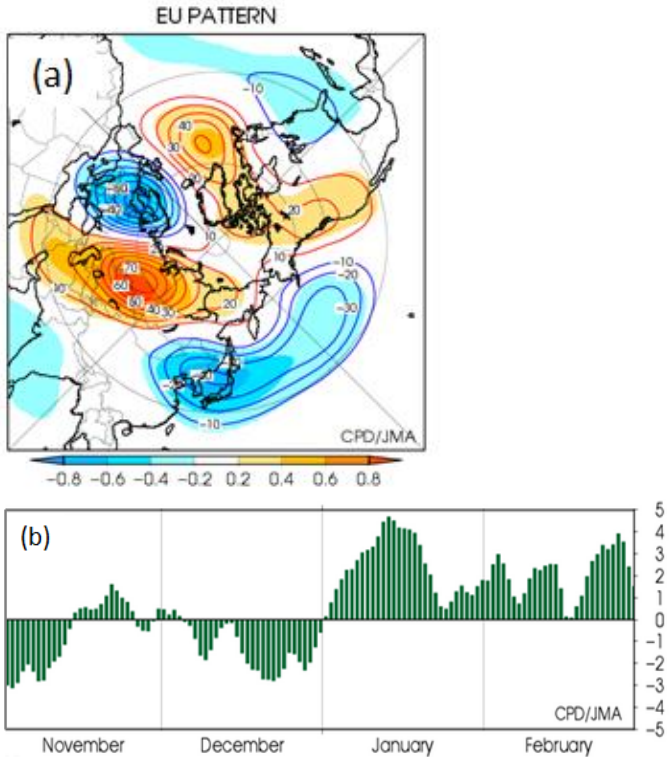

Figure 22 EU teleconnection pattern
(a) 500-hPa geopotential height anomalies regressed on EU pattern indices (contours) and correlation coefficients (shading). (b) Daily indices for November 2015 to February 2016.

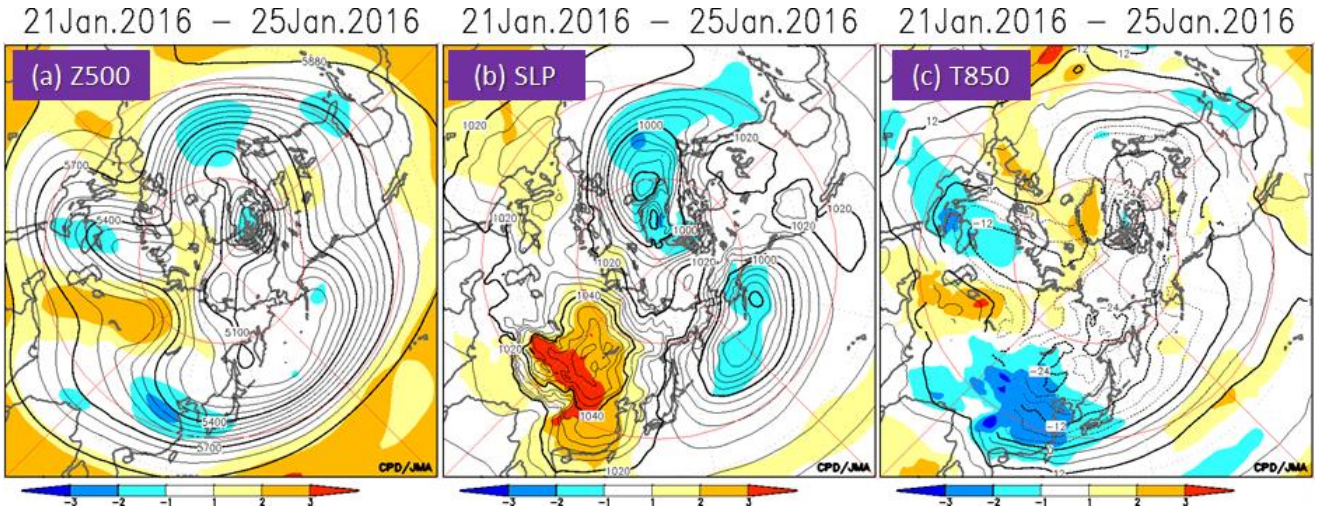

Figure 23 Circulation anomalies related to the exceptional cold wave which hit East Asia over the period of 21 – 25 January, 2016
The contours denote (a) 500-hPa height field, (b) sea level pressure field and (c) temperatures at 850-hPa. Shadings indicate related anomalies normalized by their standard deviations.

The outstanding intensity of the cold air outbreaks at that time can be evaluated using the method proposed by Iwasaki et al. (2014) in relation to cold-air mass anomalies and related horizontal flux. In this approach, the total cold-air mass below the potential temperature level of 280 K (approximately equivalent to the climatological potential temperature at 850 hPa zonally averaged along the latitude of 45°N in boreal winter) is calculated in terms of pressure difference between the ground and the 280-K level. On January 23, positive (i.e., above-normal) cold-air mass anomalies and northwesterly flux anomalies extended from eastern China toward western Japan (Figure 24 (a)). Six-hourly meridional flux anomalies of cold-air mass averaged over the 30 - 40°N and 110 - 130°E box reached their highest level since winter 1981/1982 (Figure 24 (b)), highlighting the unusual intensity of the late-January cold spell.

(Yoshinori Oikawa and Kenji Kamiguchi, Tokyo Climate Center)

References

Ishii, M., A. Shouji, S. Sugimoto and T. Matsumoto, 2005: Objective Analyses of Sea-Surface Temperature and Marine Meteorological Variables for the 20th Century using ICOADS and the Kobe Collection. Int. J. Climatol., 25, 865-879.

Iwasaki, T., T. Shoji, Y. Kanno, M. Sawada, M. Ujiie and K. Takaya, 2014: Isentropic analysis of polar cold air mass streams in the northern hemispheric winter, J. Atmos. Sci., 71, 2230-2243

Kobayashi, S., Y. Ota, Y. Harada, A. Ebita, M. Moriya, H. Onoda, K. Onogi, H. Kamahori, C. Kobayashi, H. Endo, K. Miyaoka, and K. Takahashi, 2015: The JRA-55 Reanalysis: General Specifications and Basic Characteristics. J. Meteorol. Soc. Japan, 93, 5 – 48.

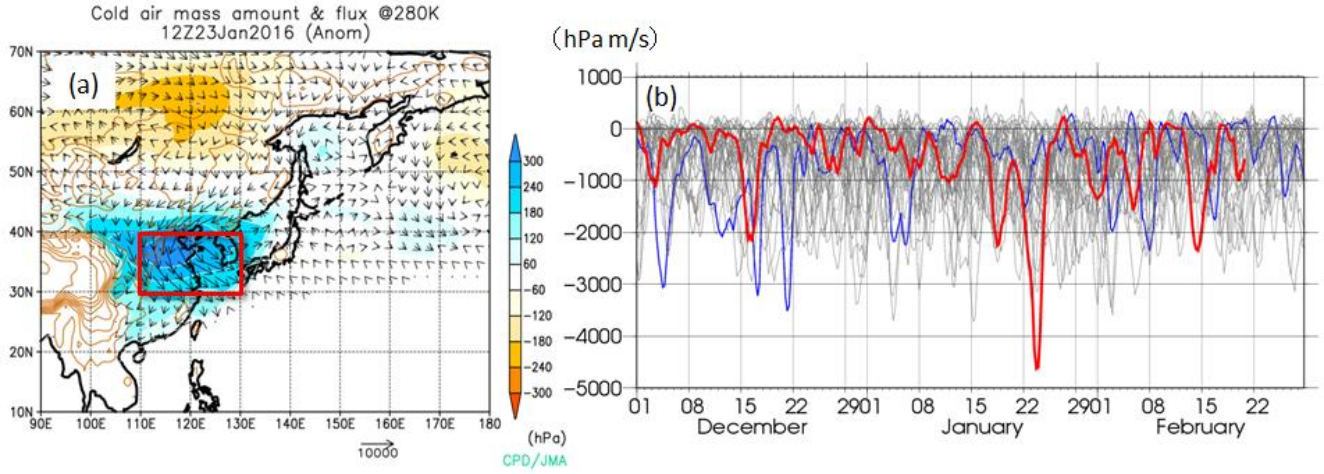

Figure 24 Intensity of cold-air masses and related flux

(a) Cold air mass amount (shading) and flux (arrows) anomalies on 12Z January 23, 2016. (b) Six hourly anomalies of cold air mass flux averaged over the box indicated in (a) for winter 2015/2016 (red), another recent cold winter 2005/2006 (blue) and other winters since 1981/1982 (grey).

TCC contributions to Regional Climate Outlook Forums in Asia

WMO Regional Climate Outlook Forums (RCOFs) bring together national, regional and international climate experts on an operational basis to produce regional climate outlooks based on input from participating NMHSs, regional institutions, Regional Climate Centers and global producers of climate predictions. By providing a platform for countries with similar climatological characteristics to discuss related matters, these forums ensure consistency in terms of access to and interpretation of climate information. In spring 2016, TCC experts participated in two RCOFs in Asia.

FOCRA II

The first RCOF was the 12th session of the Forum on Regional Climate Monitoring, Assessment and Prediction for Regional Association II (FOCRA II) in Guangzhou, China, from 7 to 9 April. At the event, experts from 12 countries/territories made presentations in six sessions featuring talks by invited lecturers and other oral presentations. TCC attendees gave three presentations on JMA's seasonal ensemble prediction system (EPS) and its output, and outlined the details of the last winter monsoon. In this way, JMA's latest seasonal predictions contributed to discussions on the consensus outlook for the coming summer.

Mr Okubo, Senior Forecaster of TCC, introduced JMA's seasonal forecast at 12th FOCRA-II.

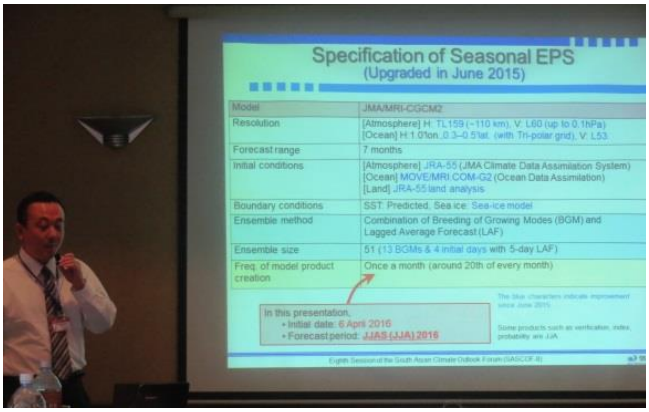

TCC experts contributed to the discussion at SASCOF-8.

SASCOF-8

The second RCOF was the eighth session of the South Asian Climate Outlook Forum (SASCOF-8) in Colombo, Sri Lanka, from 25 to 26 April. This forum, which has been held every year since 2010, provides a consensus outlook on the South Asian monsoon season. The member countries are Afghanistan, Bangladesh, Bhutan, India, the Maldives, Myanmar, Nepal, Pakistan and Sri Lanka. The SASCOF consensus outlook is important for these countries, as it helps to mitigate disasters caused by extreme climate events such as heavy rainfall and droughts. Experts from member countries shared outlooks on their own countries and engaged in discussions with global experts toward the formulation of consensus outlooks.

In order to support such activities, TCC dispatches experts annually to provide up-to-date South Asian monsoon predictions based on JMA's seasonal EPS and to contribute to discussions on the consensus outlook. At the 2016 session, Two TCC experts attended SASCOF-8 to provide predictions on oceanic and atmospheric conditions, including probabilistic forecasting of monsoon rainfall in South Asia based on JMA's seasonal Ensemble Prediction System, and briefly outlined the Center's services. The prediction was consistent with other model outputs and played an important role in the formulation of the outlook for the 2016 southwest monsoon season.

(Tadayuki Okubo, Akihiko Shimpo, Hirotaka Sato, AkioNishimura and Atsushi Goto, Tokyo Climate Center)

TCC Experts Visit Vietnam

TCC arranges expert visits to NMHSs to support climate services and the effective transfer of technology.

As part of such efforts, TCC experts visited the National Center for Hydro-Meteorological Forecasting (NCHMF) in Vietnam from 5 to 7 April 2016 to hold a training seminar regarding on the generation of one-month forecasts using the statistical downscaling technique and on the effective use of TCC's Interactive Tool for Analysis of the Climate System (iTacs). The visit was conducted as follow-up to the TCC Training Seminar of 2015 (see TCC News No.42 and TCC website for details) , and also provided a platform for discussions on future collaboration between NCHMF and TCC.

In the presence of around 18 NCHMF experts, the TCC visitors outlined the formulation of a statistical relationship between temperature and precipitation as observed in Vietnam and corresponding data from JMA's numerical prediction model. Using this relationship to downscale numerical model outputs, the attendees produced one-month forecasts for regional districts in Vietnam and then made presentations on their achievements. The TCC visitors also outlined the basic operation of iTacs via practical exercises.

The visit provided outstanding opportunities for attendees to deepen their understandings of one-month forecasting and to discuss future collaborative work with TCC. TCC will continue to arrange expert visits to NMHSs in Southeast Asia and elsewhere as necessary to assist with operational climate services.

(Yasushi Mochizuki, Tokyo Climate Center)

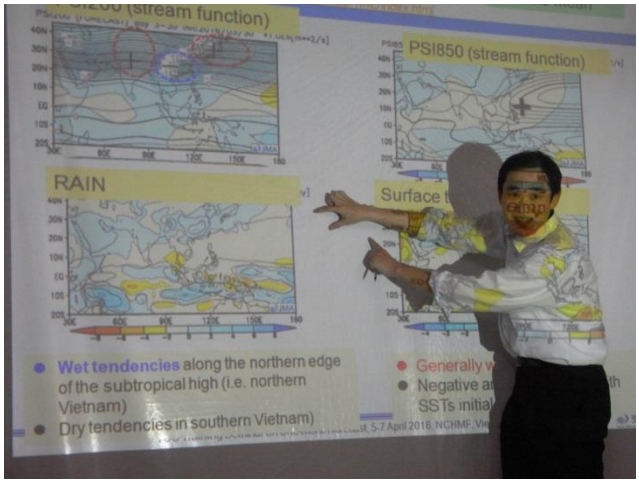

TCC website revamp

TCC provides a range of climate-related products and tools via its website to support Asia-Pacific regional and national climate services in its role as a WMO Regional Climate Center (RCC) in Regional Association II (Asia). In March 2016, the Center revamped its website to improve user accessibility and operability.

Users can now more easily access periodically updated products via the new Latest Update section on the left of the page. Positioning the mouse pointer over a window shows a key figure of each product and a related link. This upgrade provides users with convenient access to monthly, seasonally and annually updated products.

The update also provides brief introductions and links to major recommended products including iTacs (Interactive Tool for Analysis of the Climate System), long-range forecast products from the Global Producing Center (GPC Tokyo), Monthly Discussion on Seasonal Climate Outlook, El Niño Outlook, ClimatView (a worldwide CLIMAT viewer), and TCC News.

TCC updates such as product launches and TCC News releases are also provided on the upper right of the screen.

TCC maintains its commitment to supporting operational climate services at National Meteorological and Hydrological Services (NMHSs) via its website.

(Yasushi Mochizuki, Tokyo Climate Center)

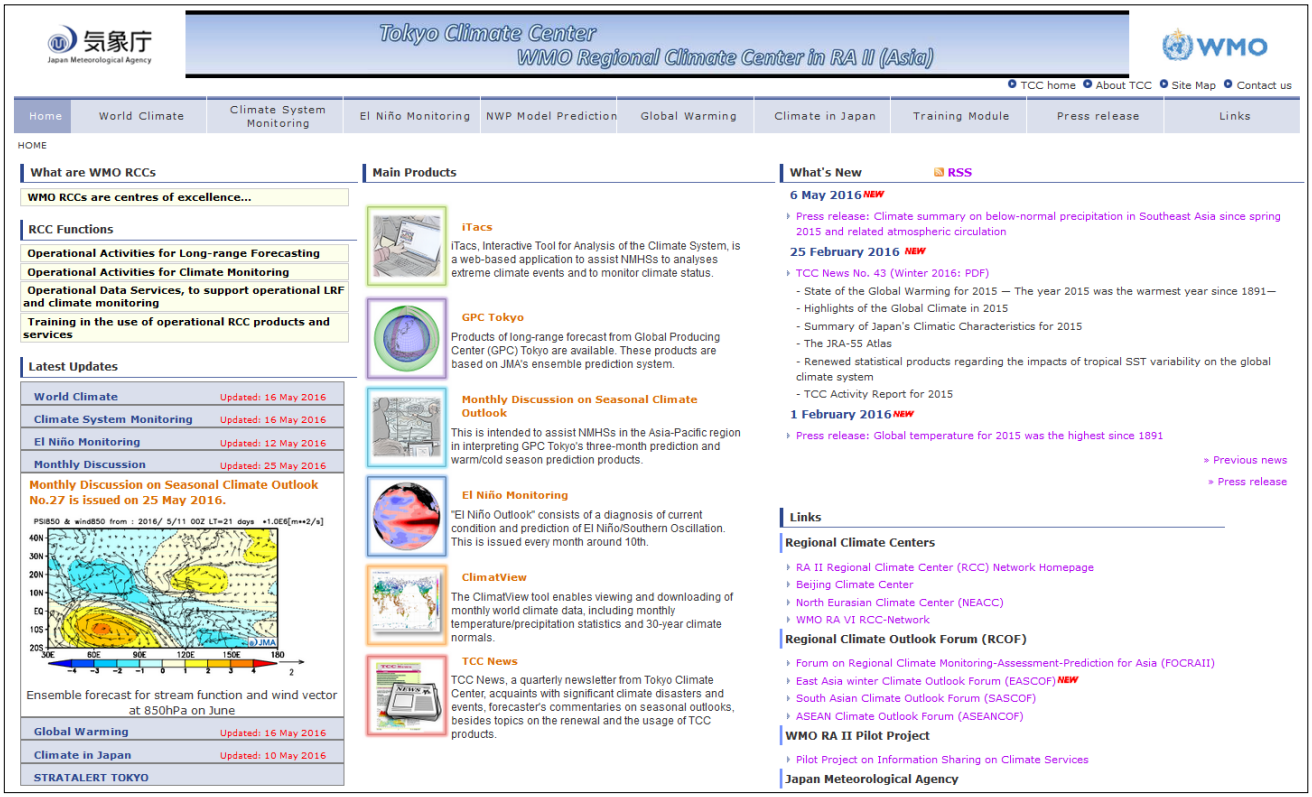

Any comments or inquiry on this newsletter and/or the TCC website would be much appreciated. Please e-mail to tcc@met.kishou.go.jp.

(Editors: Kiyotoshi Takahashi, Atsushi Goto and Yasushi Mochizuki)

Tokyo Climate Center (TCC), Japan Meteorological Agency
Address: 1-3-4 Otemachi, Chiyoda-ku, Tokyo 100-8122, Japan
TCC Website: http://ds.data.jma.go.jp/tcc/tcc/index.html